



The 2nd circular of the East-Asia AGN Workshop 2017
4-6 December 2017 in Kagoshima, Japan

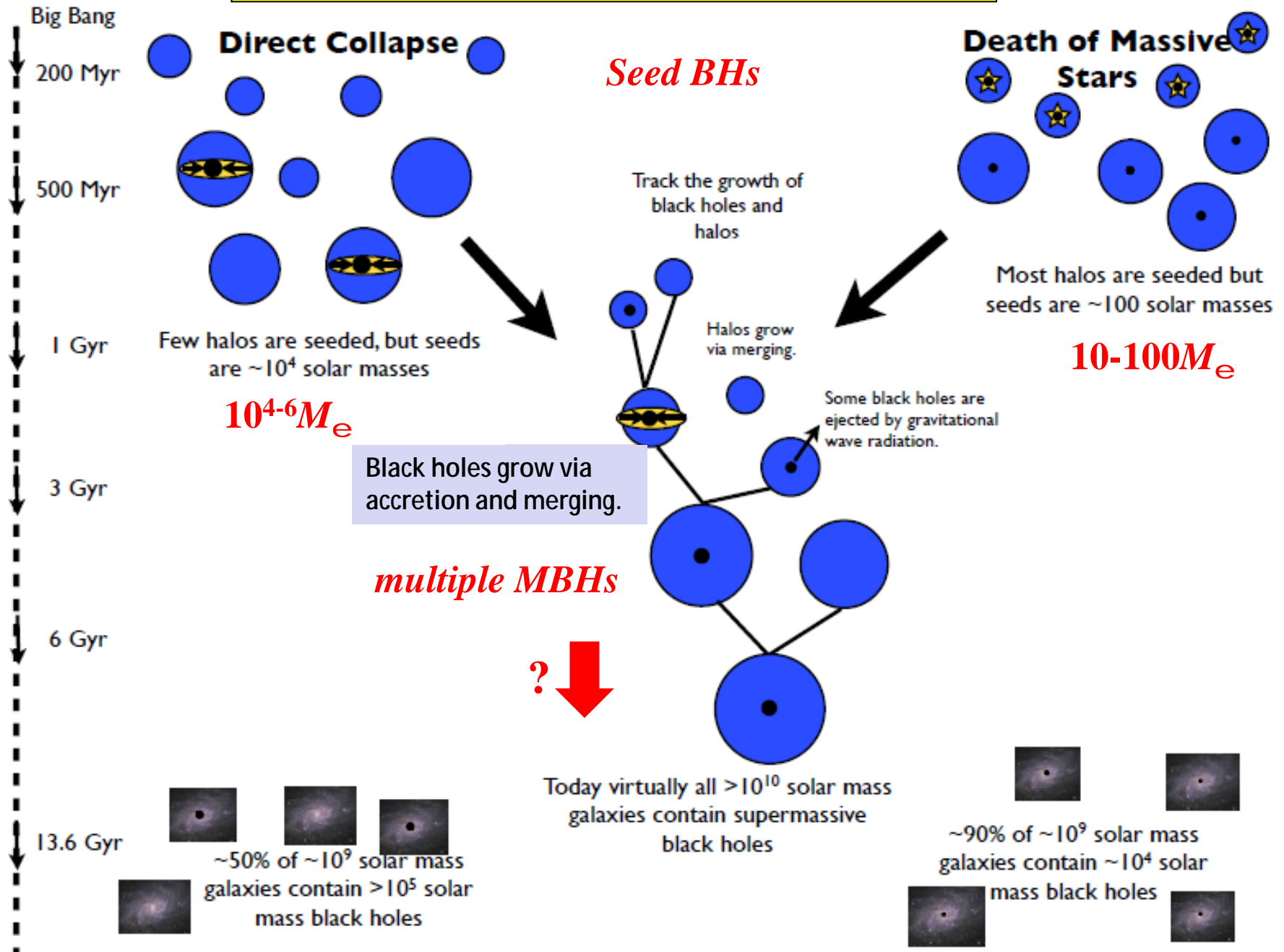
A Novel Scenario for BH mergers in Galactic Nuclei and its Relation to SMBHs

Masayuki Umemura

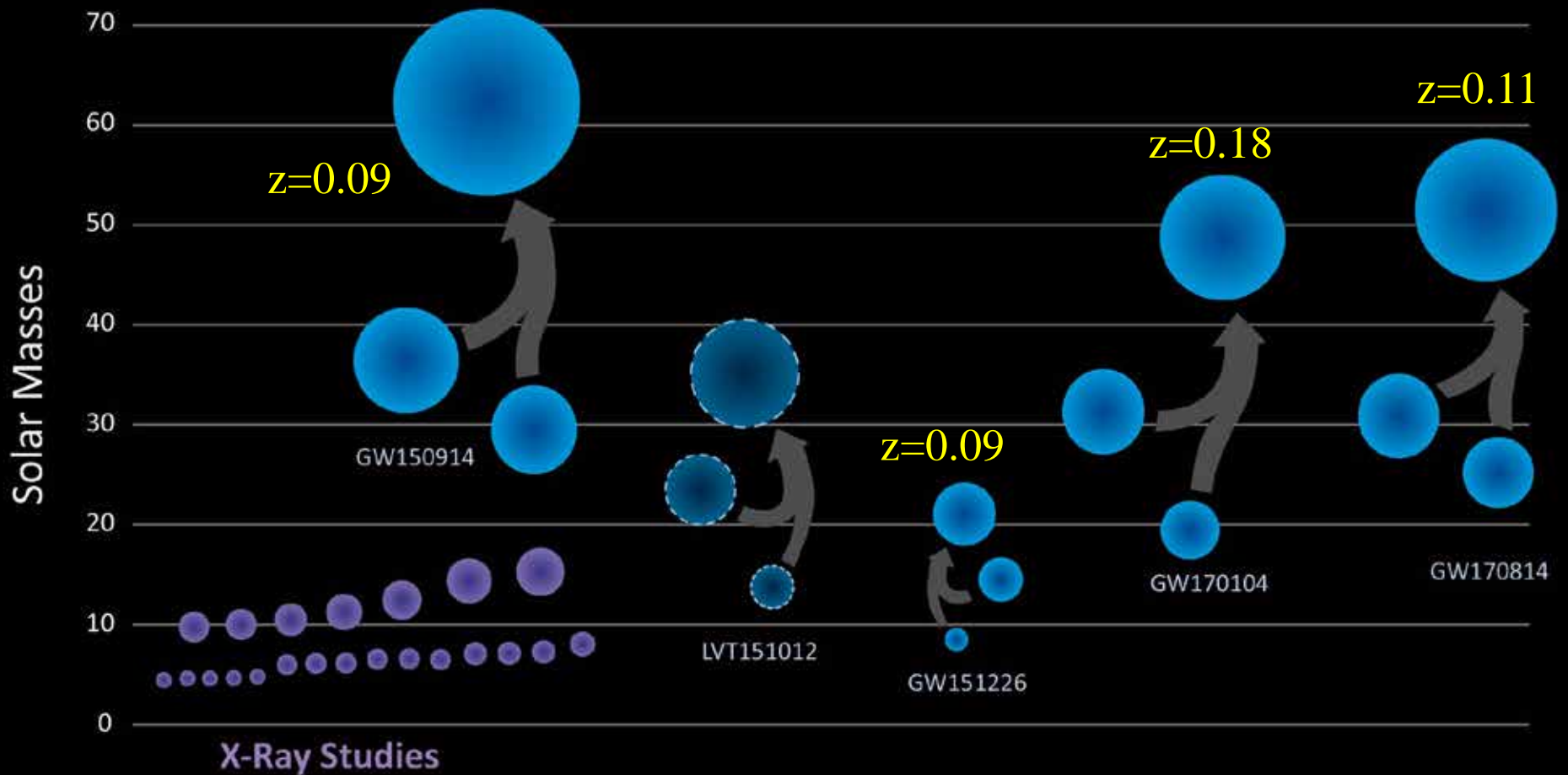
Center for Computational Sciences, University of Tsukuba

Hierarchical Growth of Massive BHs

Greene 2012



Direct Detection of BH Mergers by Gravitational Wave Radiation



BH Merger Events

GW150914

» $30M_{\oplus}$

Primary black hole mass	$36^{+5}_{-4} M_{\odot}$
Secondary black hole mass	$29^{+4}_{-4} M_{\odot}$
Final black hole mass	$62^{+4}_{-4} M_{\odot}$
Final black hole spin	$0.67^{+0.05}_{-0.07}$
Luminosity distance	410^{+160}_{-180} Mpc
Source redshift z	$0.09^{+0.03}_{-0.04}$

GW170104

» $30M_{\oplus}$

Primary black hole mass m_1	$31.2^{+8.4}_{-6.0} M_{\odot}$
Secondary black hole mass m_2	$19.4^{+5.3}_{-5.9} M_{\odot}$
Chirp mass \mathcal{M}	$21.1^{+2.4}_{-2.7} M_{\odot}$
Total mass M	$50.7^{+5.9}_{-5.0} M_{\odot}$
Final black hole mass M_f	$48.7^{+5.7}_{-4.6} M_{\odot}$
Radiated energy E_{rad}	$2.0^{+0.6}_{-0.7} M_{\odot} c^2$
Peak luminosity ℓ_{peak}	$3.1^{+0.7}_{-1.3} \times 10^{56} \text{ erg s}^{-1}$
Effective inspiral spin parameter χ_{eff}	$-0.12^{+0.21}_{-0.30}$
Final black hole spin a_f	$0.64^{+0.09}_{-0.20}$
Luminosity distance D_L	880^{+450}_{-390} Mpc
Source redshift z	$0.18^{+0.08}_{-0.07}$

GW161226

Primary black hole mass	$14.2^{+8.3}_{-3.7} M_{\odot}$
Secondary black hole mass	$7.5^{+2.3}_{-2.3} M_{\odot}$
Chirp mass	$8.9^{+0.3}_{-0.3} M_{\odot}$
Total black hole mass	$21.8^{+5.9}_{-1.7} M_{\odot}$
Final black hole mass	$20.8^{+6.1}_{-1.7} M_{\odot}$
Radiated gravitational-wave energy	$1.0^{+0.1}_{-0.2} M_{\odot} c^2$
Peak luminosity	$3.3^{+0.8}_{-1.6} \times 10^{56} \text{ erg/s}$
Final black hole spin	$0.74^{+0.06}_{-0.06}$
Luminosity distance	440^{+180}_{-190} Mpc
Source redshift z	$0.09^{+0.03}_{-0.04}$

GW170814

» $30M_{\oplus}$

Primary black hole mass m_1	$30.5^{+5.7}_{-3.0} M_{\odot}$
Secondary black hole mass m_2	$25.3^{+2.8}_{-4.2} M_{\odot}$
Chirp mass \mathcal{M}	$24.1^{+1.4}_{-1.1} M_{\odot}$
Total mass M	$55.9^{+3.4}_{-2.7} M_{\odot}$
Final black hole mass M_f	$53.2^{+3.2}_{-2.5} M_{\odot}$
Radiated energy E_{rad}	$2.7^{+0.4}_{-0.3} M_{\odot} c^2$
Peak luminosity ℓ_{peak}	$3.7^{+0.5}_{-0.5} \times 10^{56} \text{ erg s}^{-1}$
Effective inspiral spin parameter χ_{eff}	$0.06^{+0.12}_{-0.12}$
Final black hole spin a_f	$0.70^{+0.07}_{-0.05}$
Luminosity distance D_L	540^{+130}_{-210} Mpc
Source redshift z	$0.11^{+0.03}_{-0.04}$

Isolated binary BHs

(“Old playmate” scenario)

VS

Unassociated BHs

(“Chance meeting” scenario)

Isolated binary evolution (*Old playmate scenario*)

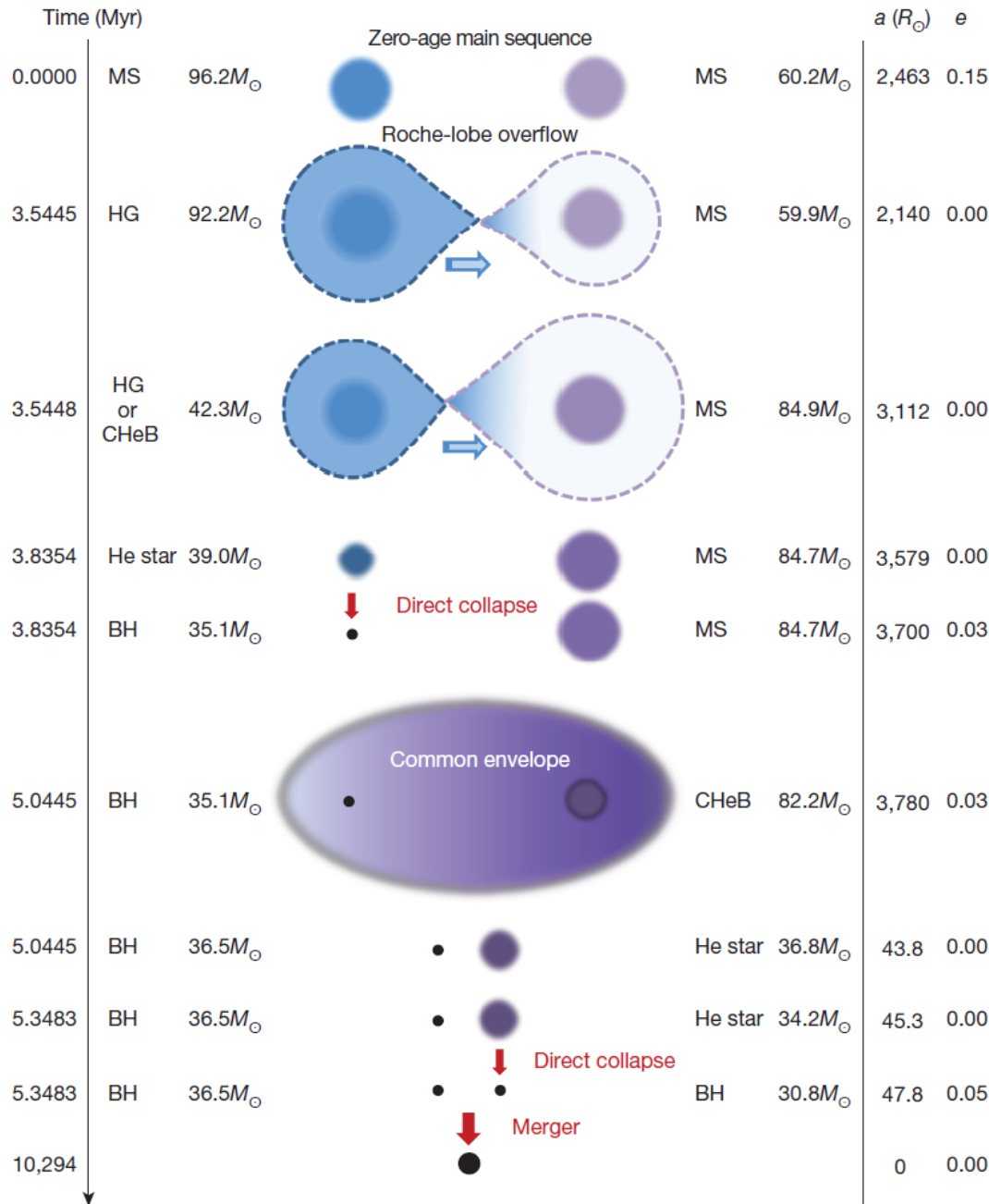


Figure 1 | Example binary evolution leading to a BH–BH merger similar to GW150914. A massive binary star ($96M_{\odot}$ (blue) + $60M_{\odot}$ (purple)) is formed in the distant past (2 billion years after Big Bang; $z \approx 3.2$; top row), and after 5 million years of evolution forms a BH–BH system ($37M_{\odot}$ + $31M_{\odot}$; second-last row). For the ensuing 10.3 billion years, this BH–BH system is subject to loss of angular momentum, with the orbital separation steadily decreasing, until the black holes coalesce at redshift $z = 0.09$. This example binary formed in a low-metallicity environment ($Z = 0.03Z_{\odot}$). MS, main-sequence star; HG, Hertzsprung-gap star; CHeB, core-helium-burning star; BH, black hole; a , orbital semi-major axis; e , eccentricity.

Belczynski et al. 2016,
nature, 534,513

also
Kinugawa et al. 2014

GW170104

Effective spin parameter

$$c_{\text{eff}} = (m_1 a_1 \cos q_{\text{LS}_1} + m_2 a_2 \cos q_{\text{LS}_2}) / M$$

$a_i = |c\mathbf{S}_i / Gm_i^2|$: dimensionless spin magnitude

$q_{\text{LS}_i} = \cos^{-1}(\hat{\mathbf{L}} \times \hat{\mathbf{S}}_i)$: tilt angle

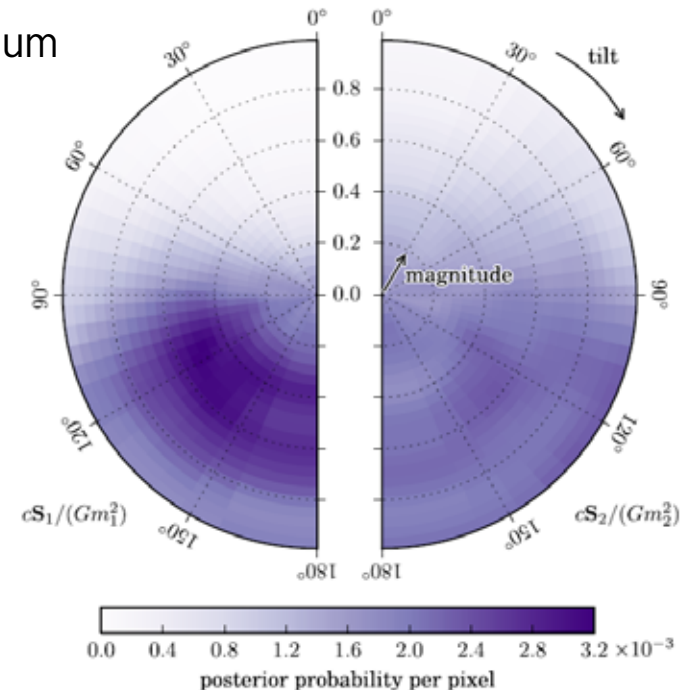
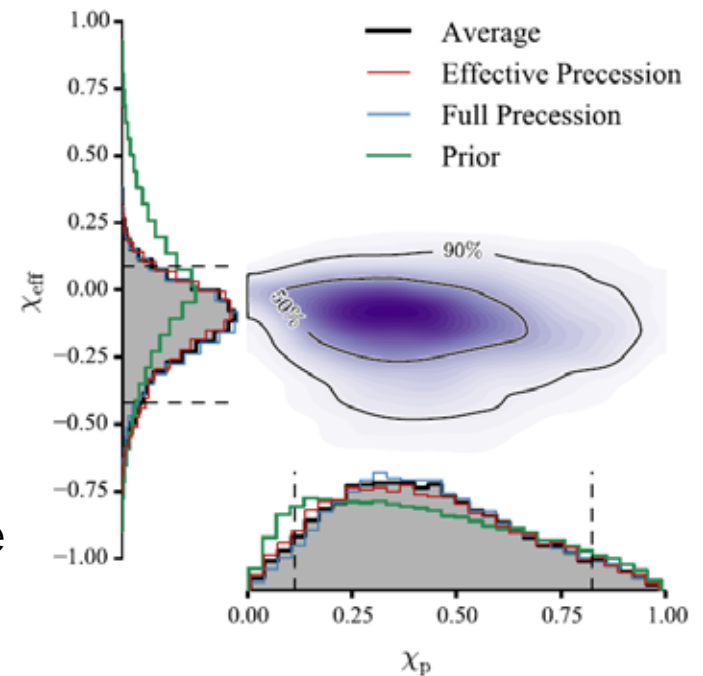
0° = spin aligned with orbital angular momentum

180° = spin antialigned

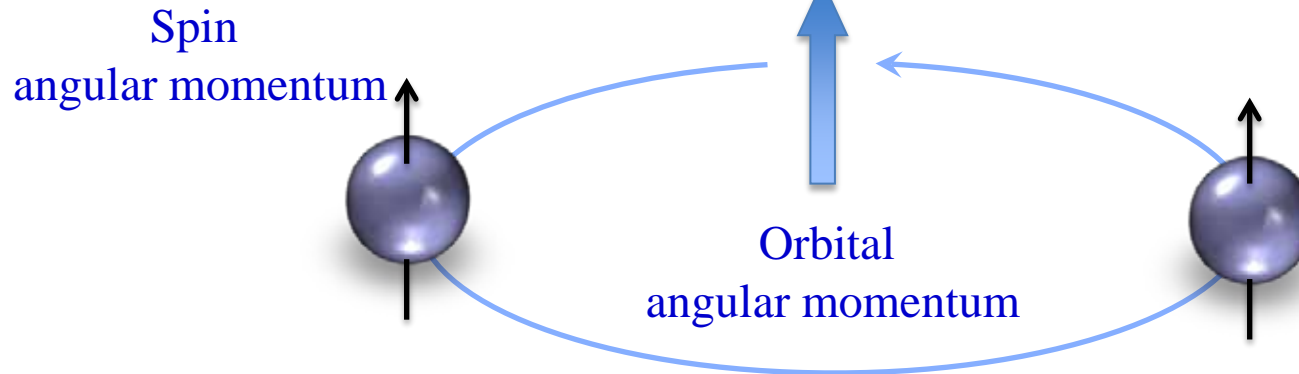
c_p single effective spin parameter

$$c_{\text{eff}} = -0.12^{+0.21}_{-0.30}$$

Spin misalignment!

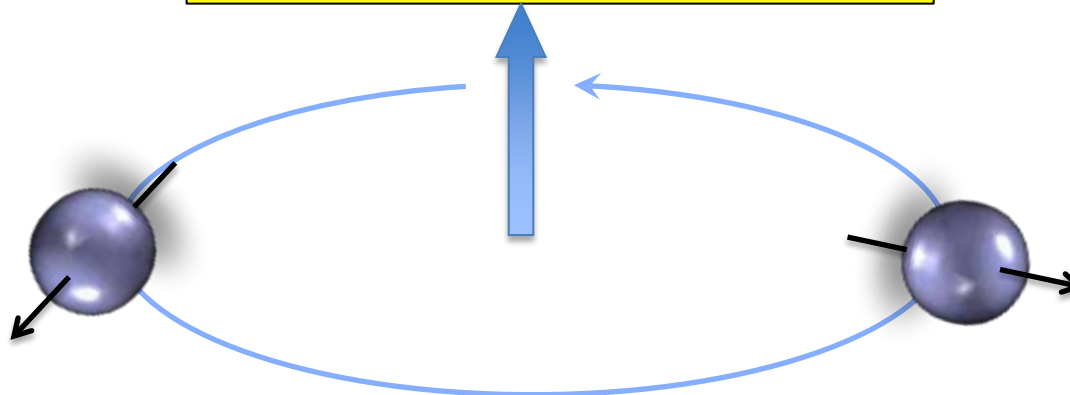


Isolated binary BH



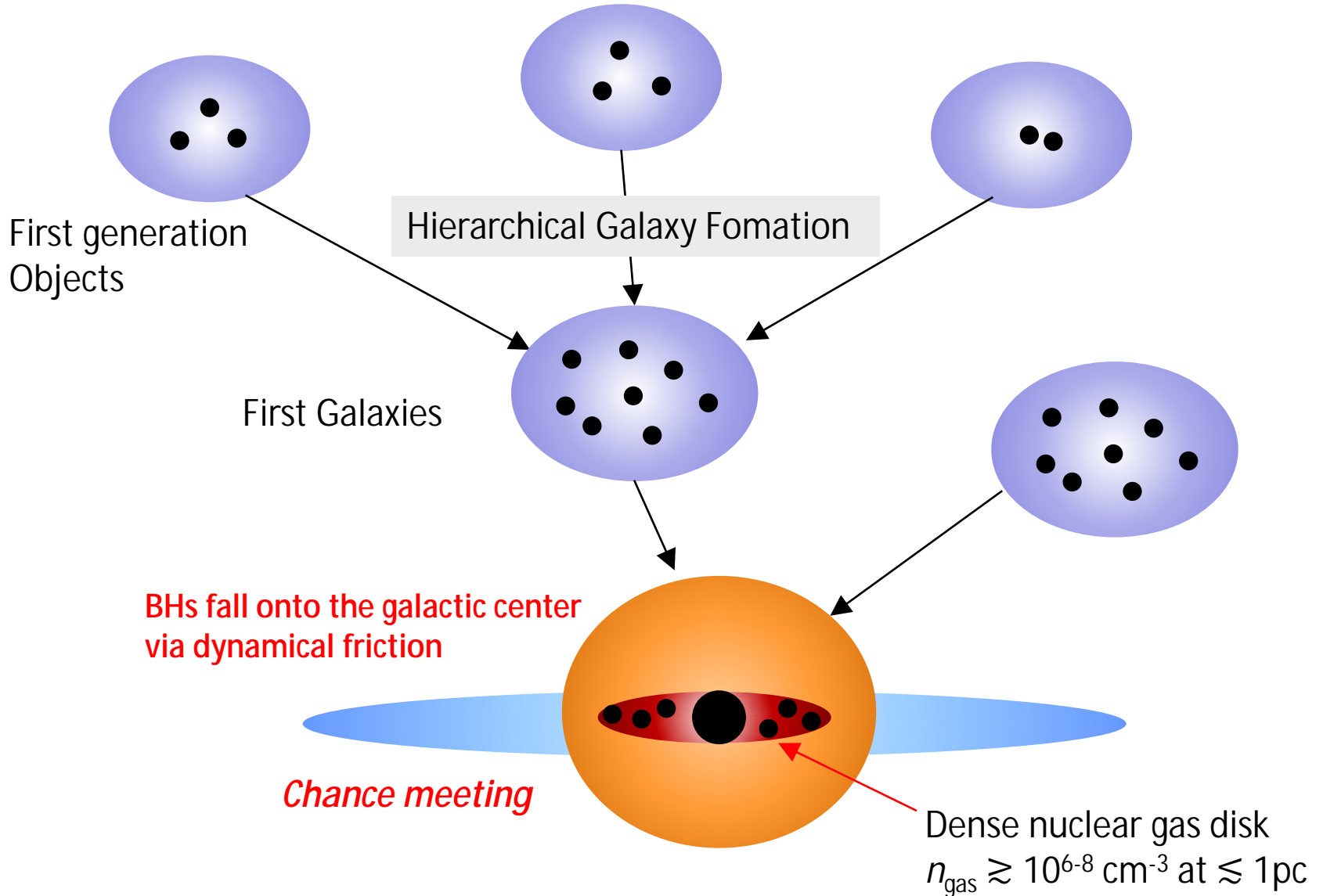
∅ Isolated binary evolution predicts spin alignments, since the effect of mass transfer and tides aligns spins with the orbital angular momentum.

Observation of GW170104

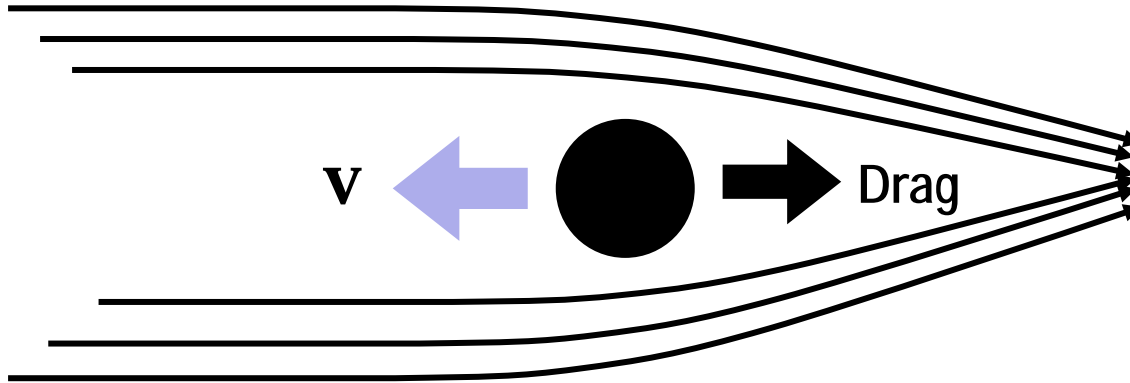


∅ The spin misalignments favor dynamically assembled BH binaries from unassociated BHs (*chance meeting*).

Scenario for BH mergers in Galactic Nuclei



Dynamical Friction by Gas



$$a_{\text{DF},i}^{\text{gas}} = -4\pi G^2 m_i m_{\text{H}} n_{\text{gas}}(r) \frac{v_i}{v_i^3} \times f(\mathcal{M}_i)$$

$$f(\mathcal{M}_i) = \begin{cases} 0.5 \ln \left(\frac{v_i t}{r_{\text{min}}} \right) \left[\text{erf} \left(\frac{\mathcal{M}_i}{\sqrt{2}} \right) - \sqrt{\frac{2}{\pi}} \mathcal{M}_i \exp\left(-\frac{\mathcal{M}_i^2}{2}\right) \right] & (0 \leq \mathcal{M}_i \leq 0.8) \\ 1.5 \ln \left(\frac{v_i t}{r_{\text{min}}} \right) \left[\text{erf} \left(\frac{\mathcal{M}_i}{\sqrt{2}} \right) - \sqrt{\frac{2}{\pi}} \mathcal{M}_i \exp\left(-\frac{\mathcal{M}_i^2}{2}\right) \right] & (0.8 \leq \mathcal{M}_i \leq \mathcal{M}_{eq}) \\ \frac{1}{2} \ln \left(1 - \frac{1}{\mathcal{M}_i^2} \right) + \ln \left(\frac{v_i t}{r_{\text{min}}} \right), & (\mathcal{M}_{eq} \leq \mathcal{M}_i) \end{cases}$$

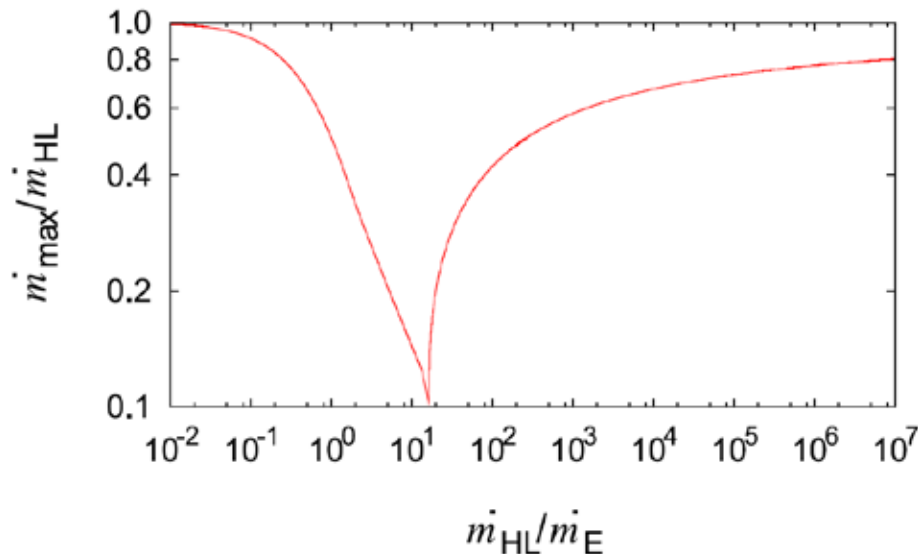
Ostriker 1999

Tanaka & Haiman 2009

Hoyle-Lyttleton accretion & Radiation pressure feedback

Hoyle-Lyttleton accretion rate

$$\dot{m}_{\text{HL}} = 4\pi r \frac{G^2 m^2}{(v^2 + c_s^2)^{3/2}}$$



Radiation pressure feedback

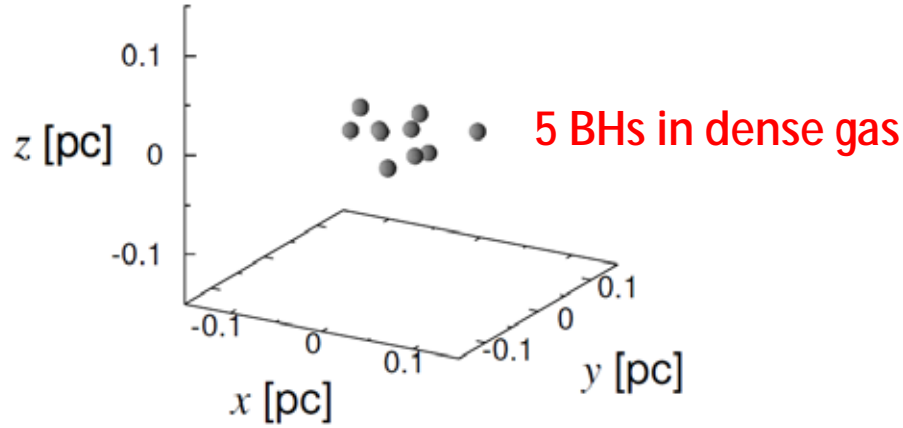
$$\frac{\dot{m}}{\dot{m}_{\text{HL}}} = \begin{cases} (1 - \Gamma) & (0 \leq \Gamma \leq 0.64) \\ (1 - \Gamma - \frac{2}{\pi} \psi_0 + \Gamma \sin \psi_0) & (0.64 \leq \Gamma \leq 1.65) \\ \frac{2}{\pi} \tan^{-1} \left(\frac{\Gamma}{0.75 \ln 10^5} \right) & (1.65 \leq \Gamma) \end{cases}$$

$G = L / L_E$: Eddington ratio

Hanamoto, Ioroi & Fukue 2001

Post-Newtonian N-body Simulation

Tagawa, Umemura, Gouda, 2016, MNRAS, 462, 3812



$$\frac{d^2 \mathbf{r}_i}{dt^2} = \sum_j^{N_{\text{BH}}} \left\{ -Gm_j \frac{\mathbf{r}_i - \mathbf{r}_j}{|\mathbf{r}_i - \mathbf{r}_j|^3} + \mathbf{a}_{\text{PN},ij} \right\} + \mathbf{a}_{\text{acc},i} + \mathbf{a}_{\text{DF},i}^{\text{gas}} + \mathbf{a}_{\text{pot},i}$$

1PN, 2PN: Pericentric shift
2.5PN: Gravitational wave

Post-Newtonian formula
by Kupi, Amaro-Seoane & Spurzem 2006

$$\mathbf{a}_{1\text{PN},ij} = \frac{Gm_j}{r_{ij}^2} \left[\mathbf{n} \left[-v_i^2 - 2v_j^2 + 4\mathbf{v}_i \mathbf{v}_j + \frac{3}{2}(\mathbf{n} \mathbf{v}_j)^2 + 5 \left(\frac{Gm_i}{r_{ij}} \right) + 4 \left(\frac{Gm_j}{r_{ij}} \right) \right] + (\mathbf{v}_i - \mathbf{v}_j)(4\mathbf{n} \mathbf{v}_i - 3\mathbf{n} \mathbf{v}_j) \right], \quad (11)$$

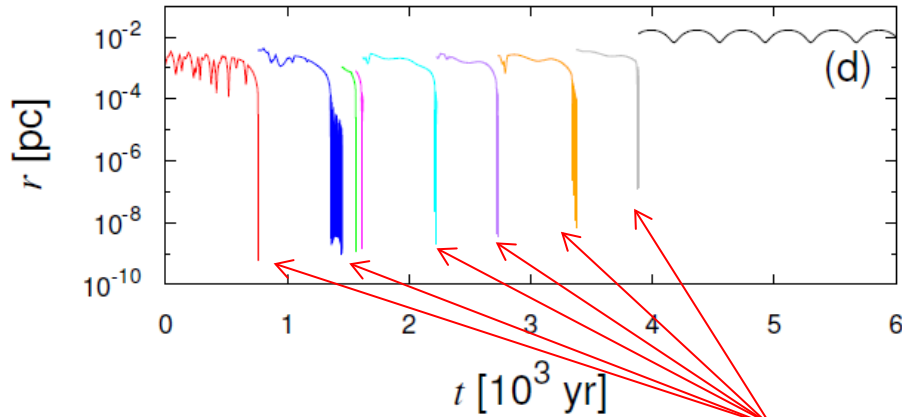
$$\mathbf{a}_{2\text{PN},ij} = \frac{Gm_j}{r_{ij}^2} \left[\mathbf{n} \left[-2v_j^4 + 4v_j^2(\mathbf{v}_i \mathbf{v}_j) - (\mathbf{v}_i \mathbf{v}_j)^2 + \frac{3}{2}v_i^2(\mathbf{n} \mathbf{v}_j)^2 + \frac{9}{2}v_j^2(\mathbf{n} \mathbf{v}_j)^2 - 6(\mathbf{v}_i \mathbf{v}_j)(\mathbf{n} \mathbf{v}_j)^2 - \frac{15}{8}(\mathbf{n} \mathbf{v}_j)^4 + \left(\frac{Gm_i}{r_{ij}} \right) \left[-\frac{15}{4}v_i^2 + \frac{5}{4}v_j^2 - \frac{5}{2}\mathbf{v}_i \mathbf{v}_j + \frac{39}{2}(\mathbf{n} \mathbf{v}_i)^2 - 39(\mathbf{n} \mathbf{v}_i)(\mathbf{n} \mathbf{v}_j) + \frac{17}{2}(\mathbf{n} \mathbf{v}_i)^2 \right] + \left(\frac{Gm_j}{r_{ij}} \right) [4v_j^2 + 8\mathbf{v}_i \mathbf{v}_j + 2(\mathbf{n} \mathbf{v}_i)^2 - 4(\mathbf{n} \mathbf{v}_i)(\mathbf{n} \mathbf{v}_j) - 6(\mathbf{n} \mathbf{v}_i)^2] + (\mathbf{v}_i - \mathbf{v}_j) \left[v_i^2(\mathbf{n} \mathbf{v}_j) + 4v_j^2(\mathbf{n} \mathbf{v}_i) - 5v_j^2(\mathbf{n} \mathbf{v}_2) - 4(\mathbf{v}_i \mathbf{v}_j)(\mathbf{n} \mathbf{v}_i) + 4(\mathbf{v}_i \mathbf{v}_j)(\mathbf{n} \mathbf{v}_j) - 6(\mathbf{n} \mathbf{v}_i)(\mathbf{n} \mathbf{v}_j)^2 + \frac{9}{2}(\mathbf{n} \mathbf{v}_j)^3 \right] + \left(\frac{Gm_i}{r_{ij}} \right) \left(-\frac{63}{4}\mathbf{n} \mathbf{v}_i + \frac{55}{4}\mathbf{n} \mathbf{v}_j \right) + \left(\frac{Gm_j}{r_{ij}} \right) (-2\mathbf{n} \mathbf{v}_i - 2\mathbf{n} \mathbf{v}_j) \right] \right] + \frac{G^3 m_j}{r_{ij}^4} \mathbf{n} \left[-\frac{57}{4}m_i^2 - 9m_j^2 - \frac{69}{2}m_i m_j \right], \quad (12)$$

$$\mathbf{a}_{2.5\text{PN},ij} = \frac{4G^2 m_i m_j}{5r_{ij}^3} \left[(\mathbf{v}_i - \mathbf{v}_j) \left[-(\mathbf{v}_i - \mathbf{v}_j)^2 + 2 \left(\frac{Gm_i}{r_{ij}} \right) - 8 \left(\frac{Gm_j}{r_{ij}} \right) \right] + \mathbf{n}(\mathbf{n} \mathbf{v}_i - \mathbf{n} \mathbf{v}_2) \left[3(\mathbf{v}_i - \mathbf{v}_j)^2 - 6 \left(\frac{Gm_i}{r_{ij}} \right) + \frac{52}{3} \left(\frac{Gm_j}{r_{ij}} \right) \right] \right], \quad (13)$$

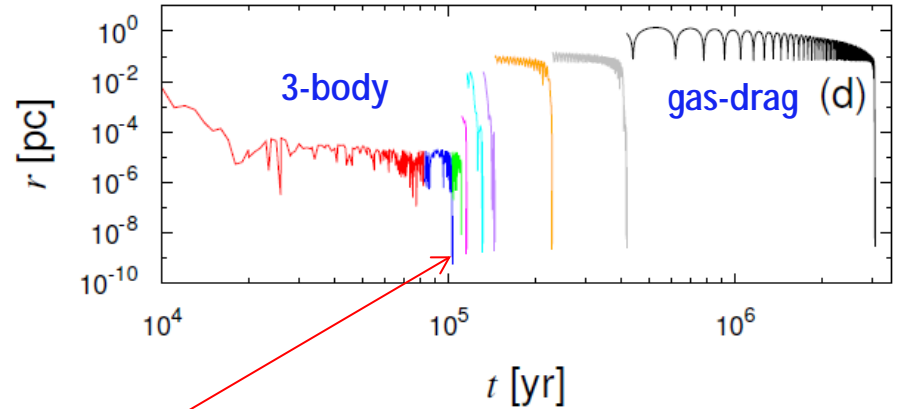
Merger of stellar-mass BHs

Tagawa, Umemura, Gouda, 2016, MNRAS, 462, 3812

Type A
Gas drag-driven merger

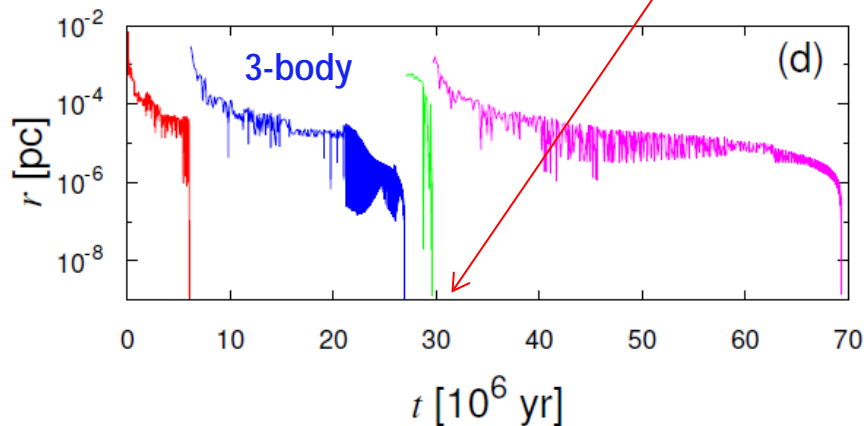


Type B
Interplay-driven merger

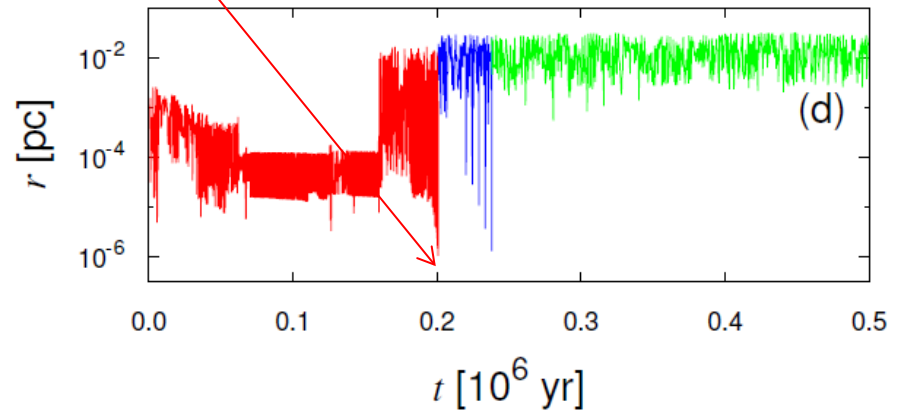


Gravitational wave emission

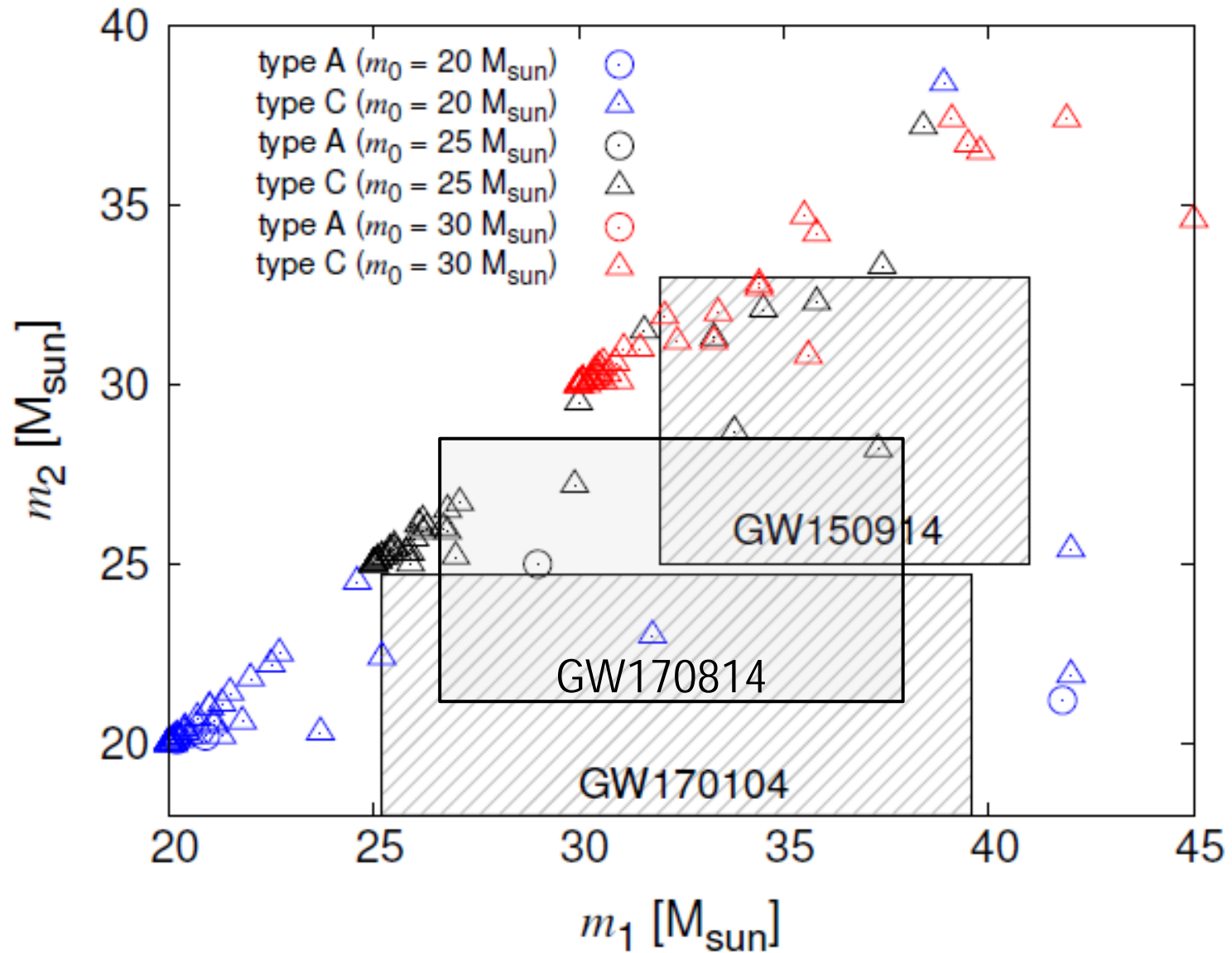
Type C
Three body-driven merger



Type D
Accretion-driven merger



$n_{\text{gas}} \gtrsim 10^{6-8} \text{ cm}^{-3} @ \lesssim 1 \text{ pc}$
(e.g. dense nuclear gas disk)



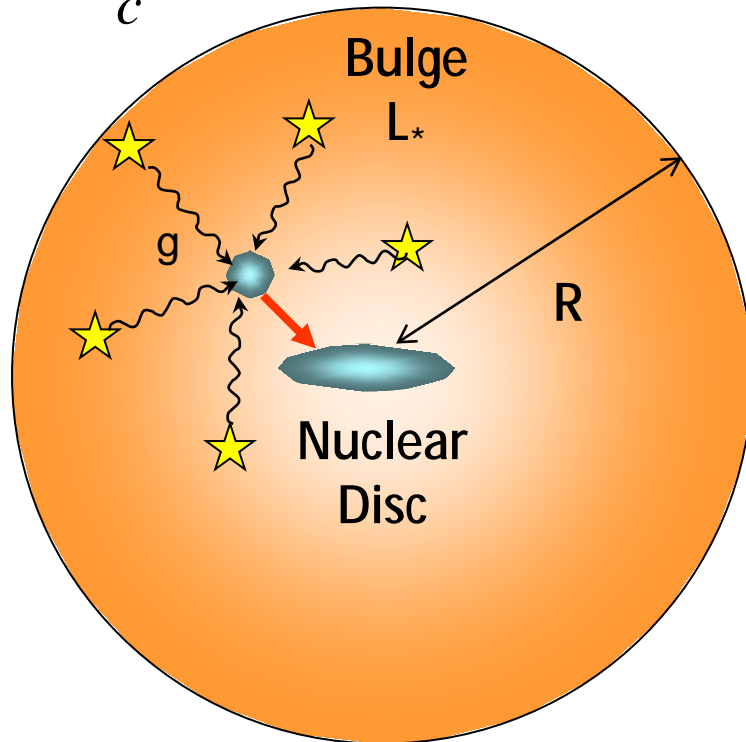
Coevolution of SMBH and Galactic Bulge

Umemura, 2001, ApJ, 560, L29

Kawakatsu & Umemura, 2002, MNRAS, 329, 572

*Poynting-Robertson Effect
in galactic bulge*

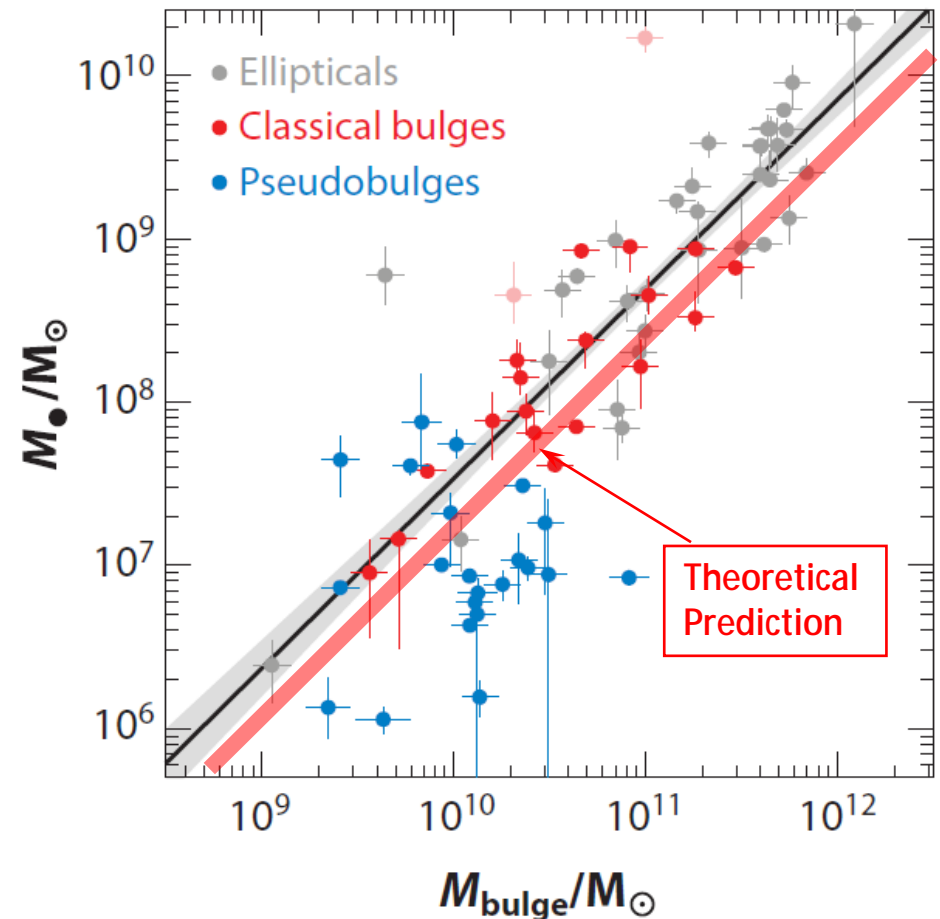
$$\dot{M} ; \frac{L_*}{c^2} (1 - e^{-t})$$



$$\frac{M_{\text{BH}}}{M_{\text{bulge}}} ; 0.14e ; 0.001$$

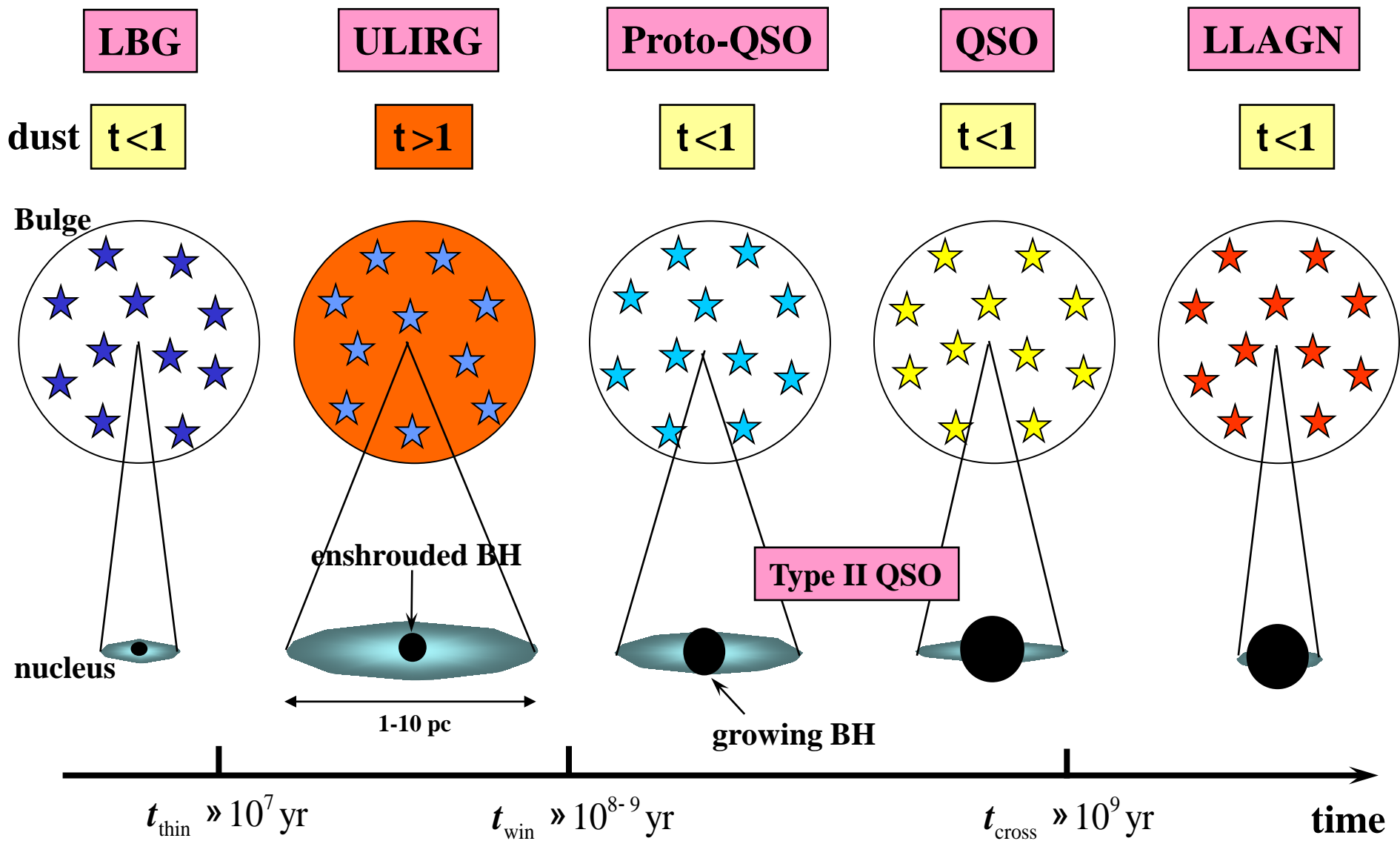
$e = 0.007$: Hydrogen burning efficiency

Kormendy & Ho 2013, ARA&A, 51, 511

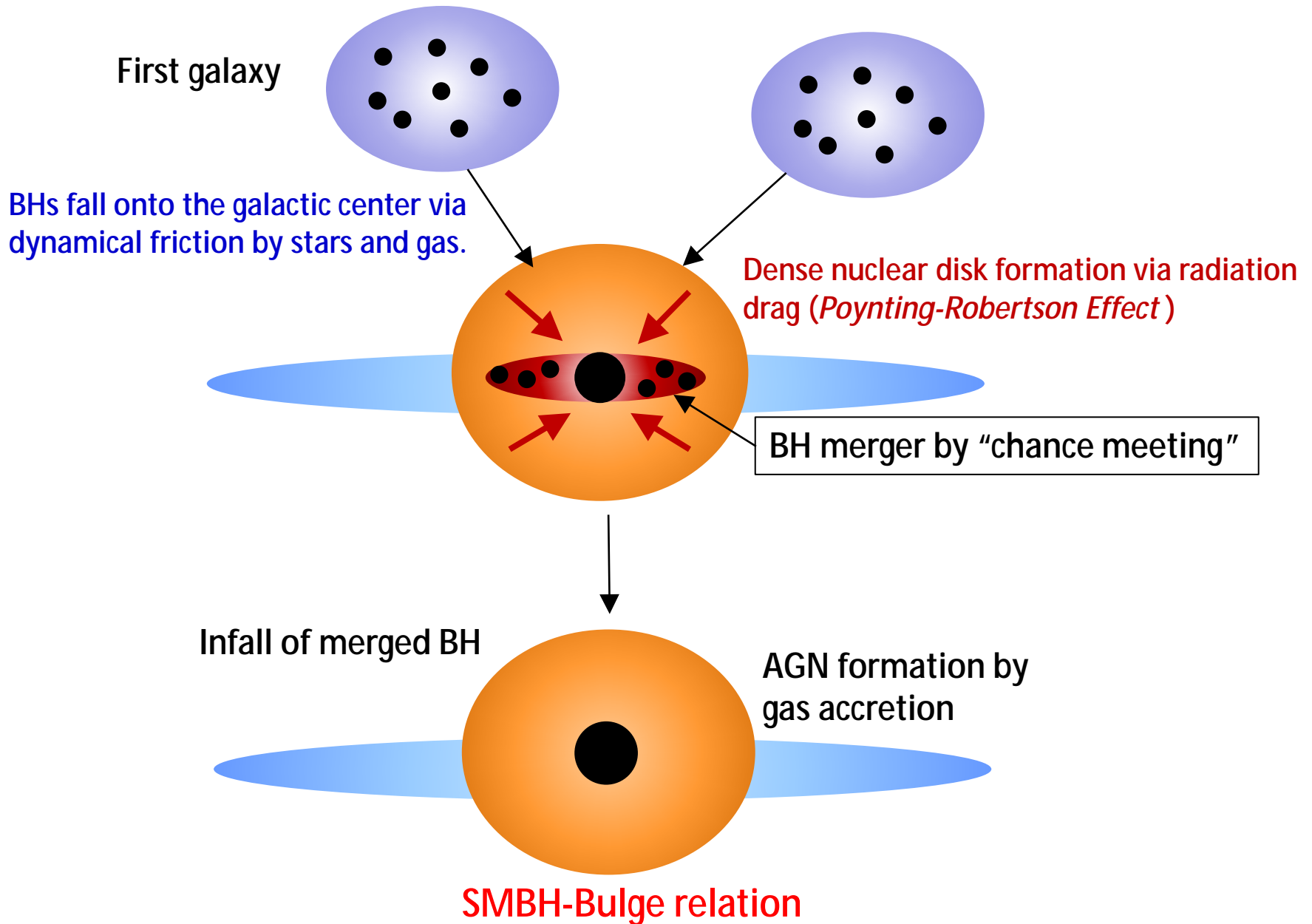


Coevolution Scenario

Umemura 2004, cbhg.sympE, 61



A Novel Scenario of Coevolution



Summary of the Scenario

- ∅ During the hierarchical galaxy formation, BHs fall onto the galactic center via dynamical friction by stars and gas.
- ∅ A nuclear dense gas disk forms via radiation drag (*Poynting-Robertson effect*) by radiation from bulge stars.
- ∅ Multiple BHs in the nuclear disk merge via “chance meeting” through gas dynamical friction and 3-body encounters within 10^8 yr.
- ∅ The merged BH falls onto the galactic center.
- ∅ An AGN is ignited by the accretion from the dense gas disk.
- ∅ Eventually, the SMBH-Bulge relation is established.